Theoret. Comput. Fluid Dynamics (1998) 10: 349–356

Theoretical and Computational Fluid Dynamics

Acoustic Streaming

N. Riley

School of Mathematics, University of East Anglia,
Norwich, Norfolk NR4 7TJ, England

Communicated by M.Y. Hussaini

Received 8 December 1996 and accepted 18 April 1997

Abstract. In this paper we discuss two types of acoustic streaming, to which Lighthill (1978a,b, 1997) has made significant contributions, namely the "quartz wind" and Rayleigh streaming. Both are associated with flows that are dominated by their fluctuating components, and owe their origin to the action of Reynolds stresses. In the former, these stresses arise within the main body of the fluid when an ultrasonic beam propagates into it; in the latter they act in the Stokes shear-wave layer that forms at a solid boundary in a fluctuating flow. In spite of its acoustic origins, we show that streaming of the Rayleigh type is a phenomenon that occurs more widely than those origins suggest.

1. Introduction

The term "acoustic streaming" has become a generic term to describe the time-averaged streaming that is induced in any fluid flow that is dominated by its fluctuating components. Its acoustic origins may be traced to the work of Rayleigh (1883, 1896). He considered the streaming motion that is induced by standing sound waves between plane walls. In more modern times streaming of another kind, often referred to as the "quartz wind", was observed when ultrasonics came into general use. Such streaming, which may be generated by any source that projects a high-intensity beam of sound into a body of fluid, was originally associated with quartz oscillators in liquids (Meissner, 1926). Both types of streaming owe their origin to the action of Reynolds stresses; and as Lighthill (1978b) points out it is the dissipation of acoustic energy flux which permits the gradients in momentum flux that force the acoustic streaming motions. In the case of the quartz wind this takes place in the main body of the fluid, whilst in Rayleigh streaming it is associated with boundary layers at solid surfaces. In this paper we build on the work of Rayleigh (1883, 1896) and Lighthill (1978a,b, 1997) to discuss both the quartz wind and the Rayleigh type of streaming. It is the latter that has implications beyond its acoustic origins.

We consider first, in Section 2, the quartz wind. A thin ultrasonic beam propagates into an unbounded volume of fluid. The Reynolds stresses are generated at second order, and are shown to represent an exponentially decaying force distributed along the jet from its origin. If the attenuation rate is sufficiently high this force becomes, for all practical purposes, a point force. For very small values of a suitably defined streaming Reynolds number, the creeping motion generated by this can be represented by a stokeslet, whilst for large streaming Reynolds number the flow assumes a jet-like character, as described by Squire (1951).

In Section 3 we discuss Rayleigh streaming that is characterized by acoustic energy dissipation within the Stokes boundary layer adjacent to a solid boundary. We develop a theory for incompressible flow, valid for large values of a suitably defined Strouhal number. The requirement of incompressibility restricts acoustic applications to situations in which $kl \ll 1$, where k is the wave number and l is a typical length. The flow region divides into an outer and inner, or Stokes-layer, region. The steady streaming originates in the latter through the direct action of Reynolds stresses, and persists at its edge (Rayleigh's law of streaming, see, for example, Lighthill (1997)). In the outer region the vorticity associated with the streaming motion is governed by a Helmholtz-type equation, but with convection of vorticity effected by the Lagrangian mean velocity, with a suitably defined streaming Reynolds number. As an example we consider the flow about a circular cylinder, induced by orthogonal sound waves which have phase difference $\frac{1}{2}\pi$, and amplitude ratio λ.

As already intimated, Rayleigh-type streaming arises in any fluid flow that is dominated by its fluctuating components, which provides for wider application than that originally associated with acoustics. Longuet-Higgin's paper (1953) of free-surface waves over a plane boundary provides a non-acoustic example. In this same context Riley and Yan (1996) and Yan and Riley (1996) have considered the flow induced about a circular cylinder beneath a free surface, over which waves propagate, on fluid of infinite depth. This finds application in ocean engineering which, as Lighthill (1995) points out, has gained special importance in the twentieth century. Lighthill himself (1991, 1992) has advanced theoretical arguments, based on the type of streaming discussed herein, to suggest that this transforms acoustic signals to neural activity, via the hair cells within the inner ear. Amongst other applications we make brief mention of only a few. Rectified diffusion is influenced by the presence of acoustic streaming (Gould, 1974; Church, 1988; Davidson, 1971). Davidson (1973) also demonstrates the significant enhancement of heat transfer, from a heated body, when acoustic streaming is present at large streaming Reynolds number, an area that has also been studied experimentally by Leung and Wang (1985). The role of acoustic streaming in acoustic levitation and positioning, to which the example of Section 3 finds application, has been studied by Busse and Wang (1981) and Lee and Wang (1988). Whilst in biophysical transport processes Secomb (1978) and Thompson (1984) have discussed the role of acoustic streaming that develops in a purely oscillatory flow field.

2. The Quartz Wind

For many, the terms "acoustic streaming" and "quartz wind" are synonymous. The streaming known as the quartz wind was observed when ultrasonics came into general use, and may be generated by any source that projects a high-intensity beam of sound into a body of fluid. It was originally, in the 1920s, associated with quartz oscillators in liquids, but subsequent observations were made in air by Walker and Allen (1950). The streaming motion is forced by the action of a Reynolds stress, but it may be noted that the gradient in momentum flux that forces this acoustic streaming is associated with the dissipation of acoustic energy flux. For the cases considered in this section, that takes place entirely within the body of fluid. An in-depth analysis of the quartz wind has only recently been given by Lighthill (1978a,b), and it is on this work that the following is based.

Consider a plane sound wave, propagating in the x-direction, from a source at $x = 0$. If non-dimensionalization is carried out with respect to time ω^{-1}, where ω is the frequency, length c/ω, where c is the sound speed, and velocity U_0, the unattenuated sound-wave velocity amplitude, then the velocity u may be shown to satisfy (Rayleigh, 1896)

$$\frac{\partial^2 u}{\partial t^2} - \frac{\partial^2 u}{\partial x^2} - \frac{4}{3}\delta\frac{\partial^3 u}{\partial x^2\,\partial t} = -\varepsilon\frac{\partial}{\partial t}\left(u\frac{\partial u}{\partial x}\right). \tag{1}$$

In (1), $\varepsilon = U_c/c$, $\delta = \omega\nu/c^2$, where ν is the kinematic viscosity; thus only the dissipative action of viscosity has been included in the "diffusivity of sound," contributions from heat conduction and irreversibility due to delays in attaining thermodynamic equilibrium have been ignored. For a further discussion, see Lighthill (1978a). Both $\varepsilon \ll 1$ and $\delta \ll 1$, and indeed these two parameters may be comparably small. However, the term $O(\delta)$ is properly included with the other linear terms of (1) if changes on the attenuation length scale, as well as on the acoustic length scale, are to be correctly incorporated.

The first-order solution of (1) is

$$u_0 = e^{-2\delta x/3}\ \cos(x - t). \tag{2}$$

The net force per unit volume contributed by the Reynolds stresses is then

$$F = -\rho U_0^2\frac{\omega}{c}\left\langle u_0\frac{\partial u_0}{\partial x}\right\rangle = \tfrac{1}{3}\rho_0 U_0^2\frac{\partial\omega}{c}e^{-4\delta x/3}, \tag{3}$$

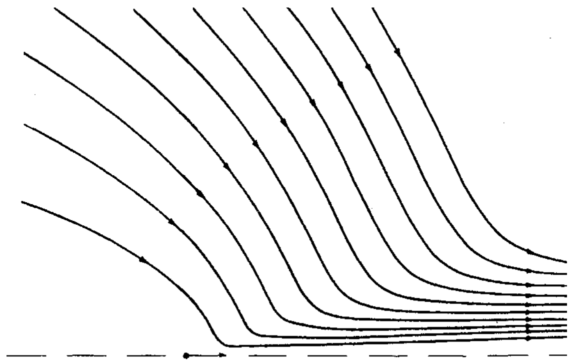

Figure 1. Streamlines for an axisymmetric jet due to a point force. $F_t/\rho\nu^2 = 3282$.

where ρ_0 is the undisturbed fluid density. For a narrow ultrasonic beam, of cross-sectional area S_b, (3) may be integrated across the beam to give the force acting, per unit length, F_l. A further integration along its length gives the total force acting, F_t. Thus

$$F_l = \tfrac{1}{3}\rho_0 U_0^2 S_b \frac{\delta\omega}{c} e^{-4\delta x/3}, \qquad F_t = \tfrac{1}{4}\rho_0 U_0^2 S_b. \tag{4a,b}$$

Now, Lighthill (1978a,b) shows that if P is the power, measured in watts, emitted by the acoustic source in a narrow beam then $F_t = P/c$ from which, using (4b), we may deduce that $U_0 = 2(P/\rho c S_b)^{1/2}$. If the total force produces acoustic streaming with typical velocity U_s in a system whose length scale is l, then $U_s = U_0 S_b/l^2 = 2(PS_b/\rho_0 c l^4)^{1/2}$ which, in turn, gives a streaming Reynolds number $R_s = U_s l/\nu = 2(PS_b/\mu\nu c l^2)^{1/2} = O(QS_b)^{1/2}$, assuming typical values for μ, ν, and c in air, with $l = 0.1$ m, for a source of $Q\,\mu$W. For $S_b^{1/2} \ll l$ and $c^3/\omega^2\nu \ll l$, corresponding to frequencies in excess of 1 MHz, the applied force is essentially a point force which may be represented as $F_t\delta(x)$.

As examples consider first the case of $Q = 1\,\mu$W, $S_b = 2\times10^{-4}$ m^2, which corresponds to $R_s = O(10^{-2})$. This is in the slow-flow regime where the applied force is resisted by viscous stresses only. In that case, on a velocity scale $F_t/8\pi\mu l$, the streaming velocity

$$\mathbf{v}^{(s)} = \left(\frac{r^2+x^2}{r^3},\ \frac{xy}{r^3},\ \frac{xz}{r^3}\right)$$

is the stokeslet velocity field. As R_s increases, with sources of greater power, the inertia terms in the governing equations become increasingly important. Ultimately the streaming flow due to the point force assumes an axisymmetric jet-like character. Such flows have been studied by Squire (1951). Lighthill (1978b) displays a sequence of such flows for increasing Q. Here, in Figure 1, we show the streamline pattern for $F_t/\rho\nu^2 = 3282$ resulting from an acoustic power source $Q = 335\,\mu$W. For a beam of cross-section $S_b = 2\times10^{-4}$ m^2 this corresponds to $R_s = O(1)$. For sufficiently high Q, and hence R_s, the induced jet flow becomes turbulent. Lighthill (1978b) presents a theory for these turbulent jets in which the point-force approximation is abandoned, and the exponential variation of the force, (4a), is accommodated.

3. Rayleigh Streaming

Streaming in the form of the quartz wind is a relatively modern phenomenon. For the origins of acoustic streaming we must push the clock back to the nineteenth century and work of Rayleigh (1883). In this work Rayleigh was concerned with the streaming induced by standing waves between plane walls. However the term "acoustic streaming" has subsequently come into general use to describe the time-averaged motion induced in any fluid flow that is dominated by its fluctuating components. Here we develop a theory for incompressible flow; the acoustic application is then associated with situations for which $kl \ll 1$, where k is the wave number and l is a characteristic length.

Suppose, then, we have a fluctuating flow, frequency ω, produced, for example, by free-surface waves or sound waves, in the presence of a solid boundary. If U_0 is again taken as the fluctuating velocity amplitude, and non-dimensionalization is carried out with respect to time ω^{-1}, length l, and velocity U_0, then Helmholtz's equation for the vorticity, in two dimensions, $\boldsymbol{\zeta} = \nabla \wedge \mathbf{v} = (0,\ 0,\ \zeta) = (0,\ 0,\ -\nabla^2\psi)$, where ψ is the stream function, is

$$\frac{\partial\zeta}{\partial t} + \frac{1}{S}(\mathbf{v}\cdot\nabla)\zeta = \frac{1}{SR_s}\nabla^2\zeta, \tag{5}$$

where $S = \omega l/U_0$ is the Strouhal number and $R_s = U_0^2/\omega\nu = U_0 a/S\nu$ will again be identified as a streaming Reynolds number, first identified as such by Stuart (1963). In what follows we develop a solution in the formal limit $S \to \infty$, with $R_s = O(1)$, and write

$$\left.\begin{aligned} \mathbf{v} &= \mathbf{v}_0 + S^{-1}\mathbf{v}_1 + \cdots\ , \\ \zeta &= \zeta_0 + S^{-1}\zeta_1 + \cdots\ . \end{aligned}\right\} \tag{6}$$

At leading order we have, from (5) and (6), $\partial\zeta_0/\partial t = 0$ from which we may infer $\zeta_0 \equiv 0$; and then we may write $\psi_0 = \psi_{0p}(\mathbf{x})e^{it}$ where ψ_{0p} is the stream function of an appropriate irrotational flow. If now, at a solid boundary, we introduce local co-ordinates (x, y) where x is measured along the boundary and y is perpendicular to it, then there is a velocity of slip

$$u = \frac{\partial\psi}{\partial y} = U(x)e^{it} \qquad \text{at} \quad y = 0. \tag{7}$$

This is corrected in the classical Stokes layer at the boundary where we write

$$\Psi = (\tfrac{1}{2}R_s)^{1/2}S\psi, \qquad Y = (\tfrac{1}{2}R_s)^{1/2}Sy \tag{8}$$

so that, from (5) and (8), we have

$$\frac{\partial}{\partial t}\left(\frac{\partial^2\Psi}{\partial Y^2}\right) - \frac{1}{S}\,\frac{\partial(\Psi, \partial^2\Psi/\partial Y^2)}{\partial(x, y)} = \frac{1}{2}\,\frac{\partial^4\Psi}{\partial Y^4} + O(S^{-2}). \tag{9}$$

As in (6), we now write

$$\Psi = \Psi_0 + S^{-1}\Psi_1 + \cdots\ , \tag{10}$$

and hence, at once, the classical Stokes-layer solution

$$\Psi_0 = U(x)[Y - \tfrac{1}{2}(1-i)\{1 - e^{-(1+i)Y}\}]e^{it}, \tag{11}$$

in which the no-slip condition is now correctly satisfied. Remaining within the Stokes layer we have, from (9) and (10), at $O(S^{-1})$,

$$\frac{1}{2}\,\frac{\partial^4\Psi_1}{\partial Y^4} - \frac{\partial}{\partial t}\left(\frac{\partial^2\Psi_1}{\partial Y^2}\right) = \frac{\partial(\partial^2\Psi_0/\partial Y^2, \Psi_0)}{\partial(x, Y)}. \tag{12}$$

The terms on the right-hand side of (12) are the Reynolds stress terms; and in this case we see that the gradient of momentum flux is associated with the dissipation of acoustic energy flux within the Stokes layer at the boundary. In solving (12) it is convenient to write

$$\Psi_1(x, y, t) = \Psi_1^{(s)}(x, Y) + \Psi_1^{(u)}(x, Y, t). \tag{13}$$

Our main concern is with the time-averaged flow induced by the Reynolds stresses, represented by $\Psi_1^{(s)}$ in (13). Taking a time average, $\langle\cdot\rangle$, of (12) and assuming that all fluctuating elements have zero time average, gives

$$\frac{1}{2}\,\frac{\partial^4\Psi^{(s)}}{\partial Y^4} = \left\langle \frac{\partial(\partial^2\Psi_0/\partial Y^2, \Psi_0)}{\partial(x, Y)} \right\rangle. \tag{14}$$

We may write the solution of (14) as

$$\Psi_1^{(s)} = \frac{d(UU^*)}{dx}f(Y) + U^*\frac{dU}{dx}g(Y), \tag{15}$$

where an asterisk denotes the complex conjugate. The functions f, g are given, for example, by Lighthill (1997). The streaming velocity created by the Reynolds stresses persists beyond the Stokes layer. Thus we have

$$\lim_{Y\to\infty}\left\{\mathrm{Re}\left(\frac{\partial\Psi_1^{(s)}}{\partial Y}\right)\right\} = u_s = -\tfrac{3}{8}\left\{(1-i)U^*\frac{dU}{dx} + (1+i)U\frac{dU^*}{dx}\right\}, \tag{16}$$

known as Rayleigh's law of streaming. The situation is, then, that the action of the Reynolds stresses within the Stokes layer drives a steady streaming beyond it, which we now investigate.

Consistent with (13) we write (6) as

$$\left.\begin{aligned} \mathbf{v}(\mathbf{x},t) &= \mathbf{v}_0(\mathbf{x},t) + S^{-1}\{\mathbf{v}_1^{(s)}(\mathbf{x}) + \mathbf{v}_1^{(u)}(\mathbf{x},t)\} + \cdots, \\ \zeta(\mathbf{x},t) &= \zeta_0(\mathbf{x},t) + S^{-1}\{\zeta_1^{(s)}(\mathbf{x}) + \zeta_1^{(u)}(\mathbf{x},t)\} + S^{-2}\zeta_2(\mathbf{x},t) + S^{-3}\zeta_3(\mathbf{x},t) + \cdots. \end{aligned}\right\} \tag{17}$$

The terms $O(S^{-1})$ in (5) give $\partial\zeta_1^{(u)}/\partial t = 0$ from which $\zeta_1^{(u)} \equiv 0$. At $O(S^{-2})$ we have $\partial\zeta_2/\partial t = -(\mathbf{v}_0\cdot\nabla)\zeta_1^{(s)}$, from which

$$\zeta_2 = -(\mathbf{v}_0^t\cdot\nabla)\zeta_1^{(s)}, \tag{18}$$

where a superscript t indicates integration with respect to time. Finally, at $O(S^{-3})$,

$$\frac{1}{R_s}\nabla^2\zeta_1^{(s)} - (\mathbf{v}_1\cdot\nabla)\zeta_1^{(s)} = \frac{\partial\zeta_3}{\partial t} + (\mathbf{v}_0\cdot\nabla)\zeta_2, \tag{19}$$

and a time-average of (19) gives

$$\frac{1}{R_s}\nabla^2\zeta_1^{(s)} - (\mathbf{v}_1^{(s)}\cdot\nabla)\zeta_1^{(s)} = \langle(\mathbf{v}_0\cdot\nabla)\zeta_2\rangle. \tag{20}$$

With ζ_2 given by (18) it may be shown that

$$\begin{aligned} \langle(\mathbf{v}_0\cdot\nabla)\zeta_2\rangle &= \{\langle(\mathbf{v}_0^t\cdot\nabla)\mathbf{v}_0\rangle\}\cdot\nabla\zeta_1^{(s)} \\ &= (\mathbf{v}_\mathrm{d}\cdot\nabla)\zeta_1^{(s)}, \end{aligned} \tag{21}$$

where

$$\mathbf{v}_\mathrm{d} = \left\langle\left(\int^t \mathbf{v}_0\,dt\cdot\nabla\right)\mathbf{v}_0\right\rangle$$

is the Stokes drift velocity. Equation (20) may then be written as

$$\frac{1}{R_s}\nabla^2\zeta_1^{(s)} - (\mathbf{v}_\mathrm{L}^{(s)}\cdot\nabla)\zeta_1^{(s)} = 0, \tag{22}$$

where $\mathbf{v}_\mathrm{L}^{(s)} = \mathbf{v}_1^{(s)} + \mathbf{v}_\mathrm{d}$. We see then, from (22), that vorticity in the outer region is convected with the mean Lagrangian velocity, and that R_s does indeed fulfil the role of a streaming Reynolds number.

Examples in which the Stokes drift velocity $\mathbf{v}_\mathrm{d}$ vanishes include the flow due to transverse oscillations of a cylinder (see, for example, Davidson and Riley, 1972), and the flow beneath standing free-surface waves over finite depth when a cylinder sits beneath a node (Wybrow *et al.*, 1996). Whilst for flows with $\mathbf{v}_\mathrm{d} \not\equiv 0$, the so-called orbital flow, we cite the examples of progressive free-surface waves over a circular cylinder for infinite fluid depth (Yan and Riley, 1996), and free-surface-wave flow over a rippled bed (Riley, 1984).

As a simple illustrative example of the foregoing we consider the situation in which plane, orthogonal sound waves, wave number k, are incident on a circular cylinder, radius a, as illustrated in Figure 2. There is a phase difference of $\frac{1}{2}\pi$ between the incident waves, their amplitude ratio is λ, and $ka \ll 1$. An alternative interpretation is that the flow is induced by the cylinder when its centre moves on an elliptic path with minor to major axes ratio λ, but maintains a fixed orientation. In that case, for $\lambda = 1$ the cylinder performs a purely orbital motion, for which a geophysical application has been advanced by Longuet-Higgins (1970), and for $\lambda = 0$ transverse vibrations along $\theta = 0$.

Following the development outlined above we have the leading-order solution

$$\psi_0 = -i\left(r - \frac{1}{r}\right)\{(\lambda-1)\,\cos\theta + e^{i\theta}\}e^{it}, \tag{23}$$

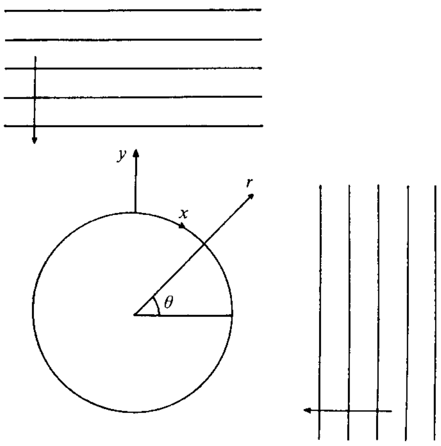

Figure 2. Definition sketch.

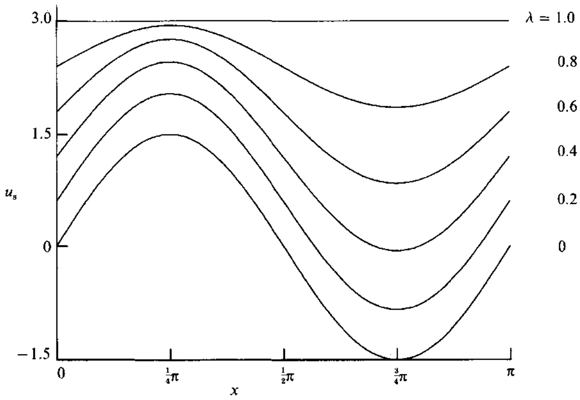

Figure 3. The slip velocity u_s, equation (25), for various values of λ.

from which, as in (7),

$$U(x) = -2i\{(\lambda - 1)\ \sin x + ie^{-ix}\}, \tag{24}$$

which, in turn, from Rayleigh's law of streaming (16), leads to a streaming velocity at the edge of the Stokes layer given by

$$u_s = \tfrac{3}{2}(1 - \lambda^2)\ \sin 2x + 3\lambda, \tag{25}$$

which is depicted in Figure 3 for various values of λ. Equation (25) provides an inner boundary condition for the solution of (22). We consider next the solution of (22); in particular we concentrate on the case $R_s \gg 1$ since, as Lighthill (1978b) has remarked, all worth-while streaming takes place at large streaming Reynolds numbers, a point that will already have been noted in Section 1. With $R_s \gg 1$ we have, from (22), $\zeta_1^{(s)} = -\nabla^2\psi_1^{(s)} = 0$, from which we deduce

$$\psi_1^{(s)} = \frac{\gamma}{2\pi}\ \log r. \tag{26}$$

In (26) the circulation γ is not uniquely determined, but we have anticipated $\gamma > 0$. The circulation may only be determined following a consideration of the flow in an outer boundary layer at the cylinder surface of thickness $O(R_s^{-1/2})$. Accordingly we write, in this boundary layer, $\tilde{y} = R_s^{1/2}y$, $\tilde{v}_1^{(s)} = R_s^{1/2}v_1^{(s)}$ so that (22) becomes

$$(\mathbf{v}_{\mathrm{L}}^{(s)} \cdot \nabla)\zeta_1^{(s)} = \frac{\partial^2\zeta_1^{(s)}}{\partial\tilde{y}} \qquad \text{where} \quad \mathbf{v}_{\mathrm{L}}^{(s)} = \{u_1^{(s)} + 2\lambda,\ \tilde{v}_1^{(s)}\},$$

or, integrating this equation once with respect to $\tilde{y}$,

$$\left.\begin{aligned} &(u_1^{(s)} + 2\lambda)\frac{\partial u_1^{(s)}}{\partial x} + \tilde{v}_1^{(s)}\frac{\partial u_1^{(s)}}{\partial\tilde{y}} = \frac{\partial^2 u_1^{(s)}}{\partial\tilde{y}^2}, \\ \text{with} \qquad &\frac{\partial u_1^{(s)}}{\partial x} + \frac{\partial\tilde{v}_1^{(s)}}{\partial\tilde{y}} = 0, \end{aligned}\right\} \tag{27}$$

the solution of which must satisfy

$$\left.\begin{aligned} &\text{at} \quad \tilde{y} = 0: \qquad u_1^{(s)} = u_s = \tfrac{3}{2}(1 - \lambda^2)\ \sin 2x + 3\lambda, \quad \tilde{v}_1^{(s)} = 0, \\ &\text{and as} \quad \tilde{y} \to \infty: \qquad u_1^{(s)} \to \frac{\gamma}{2\pi}, \\ &\text{together with the periodicity condition} \\ &\qquad\qquad u_1^{(s)}(x + 2\pi) = u_1^{(s)}(x). \end{aligned}\right\} \tag{28}$$

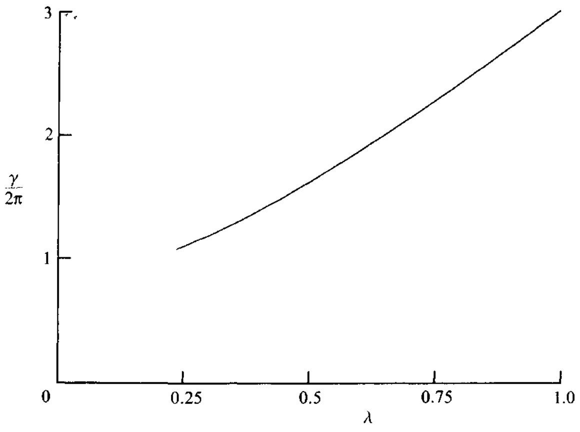

Figure 4. The circulation γ versus λ.

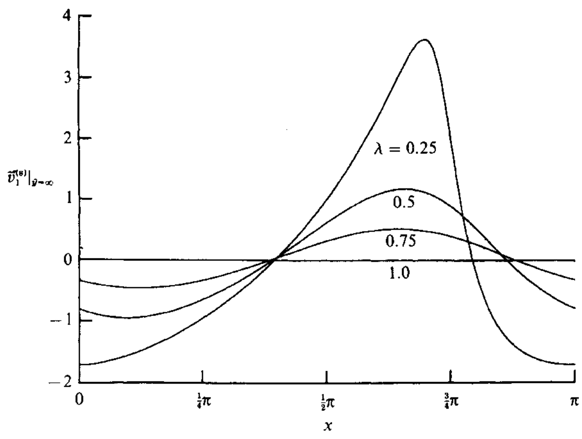

Figure 5. The normal velocity $\tilde{v}_1^{(s)}|_{\tilde{y}=\tilde{y}_\infty}$ for various values of λ.

First note that for $\lambda = 1$ the solution of (27), subject to (28), is simply $u_1^{(s)} \equiv 3$, $\tilde{v}_1^{(s)} \equiv 0$ with $\gamma = 6\pi$. In other words the Stokes layer matches directly with the outer inviscid flow without a further, intermediary, boundary layer. For $\lambda < 1$ we have completed the solution of (27), (28) numerically. Contrary to what might be thought the periodicity requirement does not determine γ uniquely for any given λ. With an outer boundary fixed for sufficiently large $\tilde{y} = \tilde{y}_\infty$, we have been able to establish a periodic solution for various values of γ. What is required, to fix γ, is that the boundary-layer solution correctly matches the outer flow, which in turn requires that $\zeta_1^{(s)} \to 0$ most rapidly as $\tilde{y} \to \tilde{y}_\infty$. To implement this requirement we minimize

$$I_\gamma = \int_0^{2\pi} \left| \frac{\partial u_1^{(s)}}{\partial \tilde{y}} \right|_{\tilde{y}=\tilde{y}_\infty} dx, \tag{29}$$

as γ varies, for a given $\tilde{y}_\infty$. As we increase $\tilde{y}_\infty$, the estimate of the required value of γ becomes sharper. The values of γ so determined are shown in Figure 4. In fact, the problem defined by (27) and (28) can be recast in the form of "Batchelor's sleeve problem" (Riley, 1992), for $\lambda > 0.28$, and $\gamma(\lambda)$ determined explicitly. The result confirms those determined from $\min(I_\gamma)$ of (29). In Figure 5 we show $\tilde{v}_1^{(s)}|_{\tilde{y}=\tilde{y}_\infty}$, for various values of λ, which may be interpreted as a measure of the displacement thickness of the boundary layer. We see a pronounced maximum in this quantity as λ decreases, and our calculations show that $\max(\tilde{v}_1^{(s)}|_{\tilde{y}=\tilde{y}_\infty}) \to \infty$, as $\lambda \to \lambda_c$, where $\lambda_c \approx 0.213$. The interpretation of this is that fluid erupts from the boundary layer and forms a jet, for $\lambda < \lambda_c$, in the manner that is well-established for the case of purely transverse vibrations, $\lambda = 0$. When there is a jet-like eruption from the streaming boundary layers the scenario set out above is inappropriate.

A characteristic feature of acoustic streaming that has emerged in both this section and Section 2 is the development of jet-like flows. The name of Lighthill is closely linked to the production of noise from jets, but the symmetry of this, with which he has also been closely associated, is the generation of jets by sound.

Acknowledgement

The author was a student at the University of Manchester during the 1950s, and acknowledges the debt he owes to Sir James Lighthill, as Beyer Professor of Applied Mathematics, for his inspirational teaching of undergraduates and leadership in research.

References

Busse, F.H., and Wang, T.G. (1981), *J. Acoust. Soc. Amer.*, Vol. 69, pp. 1634–1638.
Church, C.C. (1988), *J. Acoust. Soc. Amer.*, Vol. 84, pp. 1758–1764.
Davidson, B.J. (1971), *J. Sound Vibration*, Vol. 17, pp. 261–270.

Davidson, B.J., and Riley, N. (1972), *J. Fluid Mech.*, Vol. 53, pp. 287–303.
Davidson, B.J. (1973), *Internat J. Heat Mass Transfer*, Vol. 16, pp. 1703–1727.
Gould, R.K. (1974), *J. Acoust. Soc. Amer.*, Vol. 56, pp. 1740–1746.
Lee, C.P., and Wang, T.G. (1988), *J. Acoust. Soc. Amer.*, Vol. 83, pp. 1324–1331.
Leung, E.W., and Wang, T.G. (1985), *J. Acoust. Soc. Amer.*, Vol. 77, pp. 1686–1691.
Lighthill, M.J. (1978a), *Waves in Fluids*, Cambridge University Press, Cambridge.
Lighthill, M.J. (1978b), *J. Sound Vibration*, Vol. 61, pp. 391–418.
Lighthill, M.J. (1991), *Trans. ASME J. Vibration Acoust.*, Vol. 113, pp. 1–13.
Lighthill, M.J. (1992), *J. Fluid Mech.*, Vol. 239, pp. 551–606.
Lighthill, M.J. (1995), *Twentieth Century Physics*, Chapter 10, IOP.
Lighthill, M.J. (1997), *Handbook of Acoustics*, Chapter 27 Wiley, New York.
Longuet-Higgins, M.S. (1953), *Philos. Trans. Roy. Soc. London Ser. A.*, Vol. 245, pp. 535–581.
Longuet-Higgins, M.S. (1970), *J. Fluid Mech.*, Vol. 42, pp. 701–720.
Meissner, A. (1926), *Z. Tech. Physik*, Vol. 7, pp. 585–595.
Rayleigh, Lord (1883), *Philos. Trans. Roy. Soc. London Ser. A*, Vol. 175, pp. 1–21.
Rayleigh, Lord (1896), *The Theory of Sound*, MacMillan, London.
Riley, N. (1984), *Wave Motion*, Vol. 6, pp. 15–22.
Riley, N. (1992), *J. Fluid Mech.*, Vol. 242, pp. 387–394.
Riley, N., and Yan, B. (1996), *J. Engrg Math.*, Vol. 30, pp. 587–601.
Secomb, T.W. (1978), *J. Fluid Mech.*, Vol. 88, pp. 273–288.
Squire, H.B. (1951), *Quart. J. Mech. Appl. Math.*, Vol. 4, pp. 321–329.
Stuart, J.T. (1963), *Laminar Boundary Layers*, Chapter 7, Oxford University Press, Oxford.
Thompson, C. (1984), *J. Acoust. Soc. Amer.*, Vol. 75, pp. 97–107.
Walker, J.P., and Allen, C.H. (1950), *J. Acoust. Soc. Amer.*, Vol. 22, p. 680A.
Wybrow, M.F., Yan, B., and Riley, N. (1996) *Fluid Dynamics Res.*, Vol. 18, pp. 269–288.
Yan, B., and Riley, N. (1996), *J. Fluid Mech.*, Vol. 316, pp. 241–257.